AMERICAN SOCIETY FOR MICROBIOLOGY | Journal of Bacteriology

Microbial Genetics | Full-Length Text

SloR-SRE binding to the *S. mutans mntH* promoter is cooperative

Myrto Ziogas,[1] India Drummond,[1] Igor Todorovic,[1] Katie Kraczkowsky,[1] Yiran Han,[1] Hua Zhang,[2] Hui Wu,[2] Grace Spatafora[1]

AUTHOR AFFILIATIONS See affiliation list on p. 18.

ABSTRACT *Streptococcus mutans* is a commensal member of the plaque microbiome. It is especially prevalent when dietary sugars are available for *S. mutans* fermentation, generating acid byproducts that lower plaque pH and foster tooth decay. *S. mutans* can survive in the transient conditions of the mouth, in part because it can regulate the uptake of manganese and iron during periods of feast when metal ions are available, and famine when they are limited. *S. mutans* depends on a 25kDa metalloregulatory protein, called SloR, to modulate the uptake of these cations across the bacterial cell surface. When bound to manganese, SloR binds to palindromic recognition elements in the promoter of the sloABC genes that encode the major manganese transporter in *S. mutans*. Reports in the literature describe MntH, an ancillary manganese transporter in *S. mutans*, that is also subject to SloR control. In the present study, we performed expression profiling experiments that reveal coordinate regulation of the sloABC and mntH genes at the level of transcription. In addition, we describe a role for the mntH gene product that is redundant with that of the sloABC-encoded metal ion uptake machinery. The results of DNA-binding studies support direct SloR binding to the mntH promoter region which, like that at the sloABC promoter, harbors three palindromic recognition elements to which SloR binds cooperatively to repress downstream transcription. These findings expand our understanding of the SloR metalloregulome and elucidate SloR-DNA binding that is essential for *S. mutans* metal ion homeostasis and fitness in the oral cavity.

IMPORTANCE Dental caries disproportionately impacts low-income socioeconomic groups in the United States and abroad. Research that is focused on *S. mutans*, the primary causative agent of dental caries in humans, is significant to mitigation efforts aimed at alleviating or preventing dental caries. The SloR protein is a major regulator of the *S. mutans* metal ion uptake machinery encoded by the sloABC- and mntH genes. This SloR-mediated gene control is essential for maintaining intracellular metal ion homeostasis, and hence *S. mutans* fitness in the plaque microbiome. An improved understanding of the sloABC and mntH metal ion transporters and their regulation by SloR can guide rational drug design that, by targeting the SloR-DNA-binding interface, can alleviate or prevent *S. mutans*-induced disease.

KEYWORDS microbial genetics, cariogen, gene transcription, manganese homeostasis

The dental plaque biofilm is home to a diverse microbial community (1, 2) which includes *Streptococcus mutans*, a commensal of the healthy plaque microbiome. Stressors in the human mouth such as a high carbohydrate diet, or a change in oxygen content or pH, can give rise to dysbiotic plaque, where the microbial community is less diverse and associated with disease (3). *S. mutans* is one of the earliest colonizers of human dentition, and its prevalence on teeth is exacerbated by dietary sucrose, which strengthens the interaction of *S. mutans* with the enamel surface (4). Sucrose also serves as a substrate for *S. mutans* homolactic fermentation, the byproducts of which demineralize the tooth enamel and mark the onset of decay (5).

Editor Tina M. Henkin, The Ohio State University, Columbus, Ohio, USA

Address correspondence to Grace Spatafora, spatafor@middlebury.edu.

Myrto Ziogas and India Drummond contributed equally to this article. The two first authors on this manuscript discussed and agreed to the listed order of authorship.

The authors declare no conflict of interest.

See the funding table on p. 18.

Received 4 November 2024
Accepted 27 February 2025
Published 31 March 2025

Transition metals such as Mn^{2+} and Fe^{2+} are catalytic cofactors essential for bacterial survival and persistence in a mammalian host (6–8). Metal ion over-accumulation, however, can be toxic to cells, thereby necessitating tight regulation of metal ion uptake across the bacterial cell envelope (9). In dysbiotic plaque, *S. mutans* is a uniquely successful pathogen, in part because of its ability to maintain intracellular metal ion homeostasis despite the transient conditions of the human mouth (10). The principal metal ion uptake system in *S. mutans* is the manganese ABC-type transporter encoded by the *sloABC* operon which is modulated by SloR. SloR is a 25 kDa transcription factor that is Mn^{2+}-dependent and a member of the diphtheria toxin repressor (DtxR) family of metalloregulators. During a mealtime when foodstuffs are plentiful, Mn^{2+} is available to bind to each of three metal ion-binding sites in the SloR protein (11). This metal ion sequestration fosters SloR homodimerization and subsequent high-affinity binding of SloR to palindromic "SloR Recognition Elements," or SREs, on the DNA. Specifically, SloR-SRE binding in the *sloABC* promoter region represses downstream *sloABC* gene transcription, thereby preventing intracellular Mn^{2+} over-accumulation that could lead to cell death. During periods of famine when Mn^{2+} is limited in the mouth, *sloABC* transcription is de-repressed, which enables the cells to scavenge this essential micronutrient from the external milieu.

While manganese uptake is primarily mediated by the SloABC metal ion uptake system, Kajfasz et al. (7) recently described an ancillary transporter of manganese in *S. mutans* that works independently of, yet cooperatively with the SloABC machinery. This ancillary transporter, encoded by the *S. mutans mntH* gene, is an NRAMP-like Mn^{2+}-specific permease that, unlike the ABC-type transport that derives from the SloABC system, drives metal ion uptake via secondary active transport. In fact, the *S. mutans* MntH transporter is reminiscent of the NRAMP-like MntH permease in *Bacillus subtilis,* which is transcribed independently of the MntABCD ABC-type system (3). Kajfasz et al. also describe an important role for MntH in optimizing *S. mutans* fitness, and in particular its impact on biofilm formation and oxidative and acid stress tolerance. In that report, *mntH* is described as belonging to the *S. mutans* SloR regulon (7). Specifically, the results of semi-quantitative real-time PCR (qRT-PCR) revealed *mntH* transcription that is fivefold de-repressed in a *S. mutans* SloR-deficient GMS584 mutant compared to its UA159 wild-type progenitor. Moreover, the results of electrophoretic mobility shift assays (EMSA) support direct SloR binding to the *mntH* promoter region that harbors a predicted SRE immediately upstream of the −10 promoter element (7). Taken together, the SloR-mediated coordinate control of manganese uptake via the SloABC and MntH metal ion transport systems is likely paramount for *S. mutans* survival and persistence in dental plaque and for the cariogenic process that follows. The interaction of SloR with the *S. mutans mntH* promoter region has not been fully characterized; however, nor have the mechanism(s) that coordinate MntH- and SloABC-mediated manganese homeostasis been explored.

In the present study, we describe the promoter region of the *S. mutans mntH* gene and the SREs therein to elucidate the details of *mntH* repression by SloR. We propose at least two SREs that localize to the *mntH* promoter region to which SloR binds. We believe this binding is cooperative, involving specific base pair contacts with SloR, as well as protein interactions with the sugar-phosphate backbone. Collectively, the results of this study are consistent with the coordination of redundant SloABC and MntH metal ion transport systems via cooperative SloR binding and highlight the importance of Mn(II) homeostasis as a means to ensure *S. mutans* survival and persistence in the plaque microbiome.

MATERIALS AND METHODS

Bacterial strains, plasmids, and primers

The bacterial strains used in this study are listed in Table 1. Primers and oligonucleotides are described in Table S1 and were designed with Benchling software (2022) using the NCBI *Streptococcus mutans* UA159 genome reference sequence (RefSeq: NZ_CP007016.1). All primers and oligonucleotides were purchased from Eurofins Genomics (Louisville, KY).

Bacterial growth

S. mutans was grown as standing cultures at 37°C and 5% CO_2 in Todd-Hewitt broth (THB) or in THB supplemented with 0.3% yeast extract (THYE). THYE broth was supplemented with erythromycin (10 µg/mL) when growing *S. mutans* GMS2026, which harbors an IFDC2 cassette in the *mntH* promoter region, and with 0.02M p-chloro-phenylalanine (4 CP) when growing SRE variants GMS2027, GMS2028, and GMS2029. All variants in this study were derived from the wild-type *S. mutans* UA159 strain, using the IFDC2 markerless mutagenesis approach described in Xie et al. (12). Briefly, GMS2026 was generated by transforming UA159 cells with the IFDC2 construct and selecting for erythromycin-resistant transformants. Chromosomal DNA was isolated from these transformants and used for PCR and nucleotide sequencing to validate the incorporation of the IFDC2 cassette. Transformants were then screened for loss of the IFDC2 cassette on replica plates containing p-chloro-phenylalanine to generate SRE mutant variants GMS2027, GMS2028, and GMS2029 (12). THYE (1/4X) was used to grow *S. mutans* cells for crystal violet biofilm biomass determination assays.

^{54}Mn uptake experiments

Standing cultures of the wild-type *S. mutans* UA159 strain and its Δ*sloC*, Δ*mntH,* and Δ*sloC*/Δ*mntH* derivatives were grown in 14 mL of Todd Hewitt broth (THB) and incubated at 37°C with 5% CO_2 overnight. An amount of 250 µL of each culture was subsequently transferred to separate sterile Falcon tubes containing 45 mL of pre-warmed THB and incubated until the early exponential growth phase (OD_{600nm} = 0.1). All culture densities were normalized to within 0.005 OD units before transferring 1 mL of each culture to 1.5 mL microcentrifuge tubes and adding 1 µL of 1.8 µCi/µL ^{54}Mn (or 1 µL of 0.5 M HCl for the control). All cultures were incubated as described above for 16–18 hours, after which the cells were pelleted by centrifugation and the supernatants for each experimental sample were set aside for scintillation counting. 100 µL of each cell supernatant was transferred to vials containing scintillation fluid and assessed for counts per minute (cpm) in a liquid scintillation counter. The cell pellets from the control groups were sequentially washed in 1 mL of THB prior to resuspension. The control samples were serially diluted and plated onto THB agar plates, and viable plate counting was performed to determine the number of colony-forming units (CFU) in each sample.

TABLE 1 Bacterial strains used in this study

Strain	Relevant characteristics	Source or reference
UA159	Wild-type, serotype c	ATCC 700610
GMS2026	UA159-derived strain; contains IFDC2 cassette in the mntH promoter region; Em^r, 4-Cl-Phe^s	This study
GMS2027	GMS2026-derived; contains two A-to-C transversions in the left inverted repeat in the SRE overlapping the mntH −35 element (TTTTccGCATACTTAACA).	This study
GMS2028	GMS2026-derived; contains two transversion mutations (AG to TC) in the left inverted repeat in SRE2 (TAATtcGTACACCTTTTT) that is located immediately upstream of the mntH SRE1.	This study
UAΔsloC	UA159-derived strain; smu184::Spec	Kajfasz et al. (7)
UAΔmntH	UA159-derived strain; smu770c::Erm	Kajfasz et al. (7)
UAΔsloCΔmntH	smu184::Spec, smu770c::Erm	Kajfasz et al. (7)

Nucleic acid isolation

Chromosomal DNA and total intact RNA were isolated from *S. mutans* cells according to established protocols (13, 14).

5′ RACE

To identify the *mntH* transcription start site and predict the locale of the −10 and −35 promoter elements that drive *mntH* transcription, we performed 5′ Rapid Amplification of cDNA Ends (5′ RACE) using total RNA from *S. mutans* UA159 and an Invitrogen 5′ RACE kit (15). The primers used in this study are shown in Table S1 and include 770.GSP1.2 for reverse transcription, 770.GSP2.2 for the first round of PCR amplification, and 770.GSP3.2 for the nested PCR amplification. The reaction conditions for both PCR rounds included Platinum HiFi Taq Polymerase and a 94°C hot start, followed by a 1 minute incubation at 94°C and then 35 cycles of 94°C for 15 s, Ta for 30 s (55°C for the first round of amplification and 54°C for the second round), 68°C for 45 s, and a 4°C hold. Samples were outsourced for sequencing (Eurofins, Inc.) and results were aligned with the UA159 reference genome (RefSeq accession number NC_004350.2) using Benchling to define the transcription start site.

DNase I footprinting

DNase I footprinting was performed according to established protocols (11). A 291 bp amplicon containing the *mntH* promoter region was PCR-amplified with primers mntH.F1.fp and mntH.R1.fp. The former was end-labeled with ɣ32P-ATP and T4 polynucleotide kinase (Table S1) and the resulting amplicon was purified on a Qiaquick PCR column according to the manufacturer's instructions (Qiagen) and stored at −20°C in nuclease-free H_2O. Binding reactions were performed by combining 10 µl of 5× binding buffer (final concentration 8.4 mM NaH_2PO_4, 11.6 mM Na_2HPO_4, 50 mM NaCl, 5 mM $MgCl_2$, 10 µg/mL bovine serum albumin, 200 µg/mL salmon sperm DNA, and 7.5 µM $MnCl_2$) and up to 2 µM purified native SloR protein (11) in a 45 µL total volume. The protein and its binding buffer were incubated at room temperature for 10 minutes, after which 5 µL of radiolabeled amplicon was added. The reaction mixtures were incubated at 30°C for 30 minutes after which 5 µL of RQ1 DNase I (0.02 Kunitz units/µL) and 6 µL of 10× RQ1 reaction buffer were added for subsequent incubation at 37°C for 45 seconds. Stop solution (20 mM EGTA [pH 8.0]) prewarmed to 37°C was then added, and the reaction mixture was incubated for 10 minutes at 65°C. The DNA was purified via phenol chloroform extraction and precipitated for 5 days at −20°C in 400 µL of 100% ethanol. The DNA-protein complex was pelleted by centrifugation at 14,500 rpm for 30 minutes and 4°C and the pellets were washed in 70% ice-cold ethanol and dried for 10 minutes in a vacufuge at 30°C. The pellets were resuspended in Stop/Loading buffer (0.1% [wt/vol] bromophenol blue, 0.1% [wt/vol] xylene cyanol, 10 mM EDTA, 95% [vol/vol] formamide) before loading (2 µL per lane) on an 8% urea-containing polyacrylamide gel alongside the sequencing reactions (2.5 µL per lane). Sequencing reactions were performed with an Affymetrix Thermo Sequenase Cycle Sequencing Kit in accordance with the manufacturer's instructions for radio-labeled primer cycle sequencing (USB, Cleveland, OH). The DNA footprint was resolved for 1.5 hours at 1,600 V, after which the gel was loaded a second time and run for an additional 1.5 hours. The gel was exposed to Kodak BioMax film for up to 24 hours at −80°C in the presence of an intensifying screen before it was developed by autoradiography.

Electrophoretic mobility shift assays

EMSAs were performed using established protocols (15) to define the region in the *mntH* promoter to which SloR binds. Primers or oligonucleotides were designed to generate individual target probes that collectively span the 206 bp *mntH* promoter region or derivatives thereof. PCRs with Q5 High-Fidelity DNA polymerase (New England BioLabs) were used to amplify the target probes from the *S. mutans* UA159 chromosome.

Amplicons were confirmed by agarose gel electrophoresis and purified with a Qiagen PCR Purification Kit (Thermo Fisher, Waltham, MA) prior to end-labeling with γ−32P-ATP in the presence of T4 polynucleotide kinase (New England BioLabs). Single-stranded oligonucleotides were annealed according to established protocols before end-labeling (16).

Binding reactions were prepared as described previously (15) in a 16 µL reaction volume containing purified native SloR protein (10 µg/mL) at concentrations ranging from 60 nM to 200 nM. EDTA was added to select reaction mixtures at a final concentration of 15 mM to confirm that SloR-DNA binding was Mn-dependent. A reaction mixture containing a target probe on which the *sloABC* promoter is resident was used as a positive control for SloR binding (7, 17). The samples were loaded onto 12% nondenaturing polyacrylamide gels and run for 450 to 600 Volt-hours depending on the length of the DNA probe. Gels were exposed to Kodak BioMax film for up to 5 days at −80°C in the presence of an intensifying screen for subsequent autoradiography.

Construction of *S. mutans mntH* SRE variant strains

To introduce site-specific mutations into the *mntH* promoter region, we used *S. mutans* UA159 and a markerless mutagenesis approach described previously by Xie et al. (12). Specifically, we performed overlap extension PCR (OE-PCR) to generate a linear construct that contained a 2.2 kb IFDC2 cassette with homologous arms that flank the *mntH* promoter region. This construct was transformed into *S. mutans* UA159 with competence-stimulating peptide (CSP) and integrated into the chromosome via allelic exchange to generate GMS2026, an erythromycin-resistant and *p*-4-chlorophenylalanine (*p*-Cl-Phe) -sensitive derivative. The double-crossover event was confirmed by PCR and Sanger sequencing. A derivative of GMS2026 was subsequently generated by introducing two point mutations into *mntH* SRE1 followed by allelic exchange into the GMS2026 chromosome (Table S1). The mutated OE-PCR construct was prepared with a degenerate primer set harboring A→C mutations that localize to the leftmost inverted repeat of SRE1 upstream of the *mntH* −35 promoter. Incorporation of this mutation into the *S. mutans* chromosome at the locale of "SRE1" was validated by Sanger sequencing, and the resulting strain was called GMS2027. In a parallel set of experiments, two other GMS2026 derivatives were generated as OE-PCR constructs containing two transversion mutations in the leftmost hexameric repeat of so-called "SRE2" (TAATAGGTACACCTTTTT to TAATtcGTACACCTTTTT) or mutations in both SRE1 and SRE2. The resulting mutant variants were named GMS2028 and GMS2029, respectively.

Semiquantitative real-time PCR (qRT-PCR)

To assess the impact of SRE mutations on downstream *mntH* transcription, we isolated total intact RNA from *S. mutans* UA159, GMS2027, GMS2028, and GMS2029 cultures grown to the mid-logarithmic phase in THYE (the UA159-derived mutant variants were grown in a medium supplemented with *p*-4-chlorophenylalanine). RNA quality was assessed on an Agilent Bioanalyzer before reverse transcribing 100 ng of each RNA into cDNA. The cDNAs were used as templates in qRT-PCR experiments performed in a CXR thermal cycler (Bio-Rad) according to established protocols (16). The expression of *mntH* was measured in each of three independent experiments, each performed in triplicate and normalized against the expression of an *hk11* gene, which did not change under the experimental test conditions (18).

Phenotypic characterization of *S. mutans mntH* mutant strains

Crystal violet release assays

Overnight cultures of *S. mutans* UA159, its isogenic *mntH*, *sloC*, and *mntH/sloC* insertion-deletion mutants were all grown to the mid-logarithmic phase (OD_{600nm} of 0.4–0.6) in THYE medium at 37°C and 5% CO_2. The cells were centrifuged at 7,000 rpm for 4 minutes and the resulting pellets were resuspended in 10 mL of 1/4 strength THYE (to

encourage subsequent biofilm formation) containing 18 mM glucose and 2 mM sucrose. The resuspended cultures were used to inoculate a 24-well polystyrene microtiter plate (Corning, New York, USA) containing fresh 1/4× THYE medium as described above. The microtiter plates were incubated for 18 hours to allow for biofilm formation, and then agitated gently for 5 minutes on a Gyrotory Shaker-Model D2 rotating platform (New Brunswick Scientific Company, NJ, USA) set at 100 rpm to dislodge non-adherent cells. Culture supernatants were decanted by gentle inversion, and the biofilms were washed once with 2 mL of water. 500 µL of crystal violet (0.1% wt/vol) was then added to each well, and the plates were incubated standing at room temperature for 15 minutes. Excess crystal violet was removed from the wells by gentle inversion, and the wells were washed twice with 1 mL of water before they were air-dried for 1 hour. Intracellular crystal violet was extracted from the adherent cells in 2 mL of 99% ethanol and absorbance was measured at 575 nm in a Genesys 20 spectrophotometer (Thermo Scientific). Wells containing uninoculated 1/4× THYE were included in the experimental design and used as negative controls.

Growth determination assays

Overnight cultures of *S. mutans* UA159 and its mutant derivatives were grown to the mid-logarithmic phase (OD_{600nm} 0.4–0.6). Final cell culture densities were standardized to within 0.05 OD units with fresh THYE broth before inoculating microtiter wells (1:100) in duplicate in THYE medium. Growth was monitored at 600 nm over a 24 hour period in a BioScreen C Microplate Reader (Thermo Labsystems) according to the manufacturer's instructions.

Scanning electron microscopy

Overnight cultures of *S. mutans* UA159 and its mutant derivatives were grown to the mid-logarithmic phase (OD_{600nm} 0.4–0.6) in THYE medium as described above. Biofilm growth was initiated by inoculating mid-logarithmic phase cells into the wells of a 24-well polystyrene microtiter plate, each containing fresh THYE medium and sterile Thermanox coverslips (Electron Microscopy Sciences). The biofilms were grown for 18 hours at 37°C and 5% CO_2, washed once in 10 mM phosphate-buffered saline (PBS), fixed at room temperature in 2 mL of 3.7% formaldehyde in 10 mM PBS for 24 hours, and then dehydrated in ethanol rinses prior to air drying. All samples were sputter coated with a gold-palladium mixture and then examined with a Tescan Vega 3 LMU scanning electron microscope (Brno, Czech Republic).

Biolayer interferometry

Biolayer interferometry (BLI) was performed using the Octet Red96 system (FortéBio, Fremont, CA) as previously described (19). In brief, kinetic binding assays were performed at 30°C with a shaking speed of 1,000 rpm in a 384-well plate. Each well contained 60 µL of PBS (pH 7.2) supplemented with 0.1% Tween-20 and 100 µM $MnCl_2$. Purified SloR protein in PBS (pH 7.2) was immobilized on an NTA biosensor, followed by the application of a series of diluted synthesized oligonucleotide probes through the protein-coated biosensors. Binding interactions between SloR and the probes were analyzed using the Octet Red System Data Analysis software.

RESULTS

The *S. mutans* MntH and SloABC manganese transport systems are redundant and compensatory

To elucidate the relative contribution of MntH-mediated Mn^{2+} transport to total intracellular manganese in *S. mutans*, we conducted ^{54}Mn uptake assays with the UA159 wild-type strain and its derivatives harboring mutations in genes that encode metal ion transport. Specifically, these assays monitored cpm in culture supernatants across strains from which relative intracellular ^{54}Mn concentration could be inferred. Specifically, the

cpm in culture supernatants of *S. mutans* UA159 was compared with that of its *ΔmntH*, *ΔsloC,* and *ΔmntHΔsloC* derivatives and used as a proxy to infer intracellular cpm in cell pellets. The experimental findings support a significantly heightened accumulation of ^{54}Mn in supernatants of the *ΔmntHΔsloC* double mutant compared to the UA159 wild-type and *ΔsloC* strains (Fig. 1, $P < 0.05$, $N = 3$), consistent with compromised metal ion uptake in the double mutant and the essentiality of the MntH and SloABC transport systems in *S. mutans* manganese import. A compensatory role for manganese transport via the SloABC and MntH systems is also implicated by ^{54}Mn accumulation that did not differ significantly in the supernatants of the *ΔmntH* and *ΔsloC* single mutants.

To determine whether compensatory roles for the *mntH* and *sloABC* systems could be demonstrated at the level of phenotype, crystal violet release assays were performed to assess the biofilm biomass of the *S. mutans* wild-type and mutant strains. These experiments were performed in parallel with scanning electron microscopy imaging to monitor the details of biofilm architecture in these strains. Growth determination assays were also performed to ensure similar rates of growth for *S. mutans* UA159 and its isogenic Δ*mntH, ΔsloC,* and *ΔmntHΔsloC* manganese uptake mutants. The results of growth determination assays confirmed similar doubling times (90 minutes) for all test strains (data not shown). Crystal violet assays revealed a significant reduction in biofilm

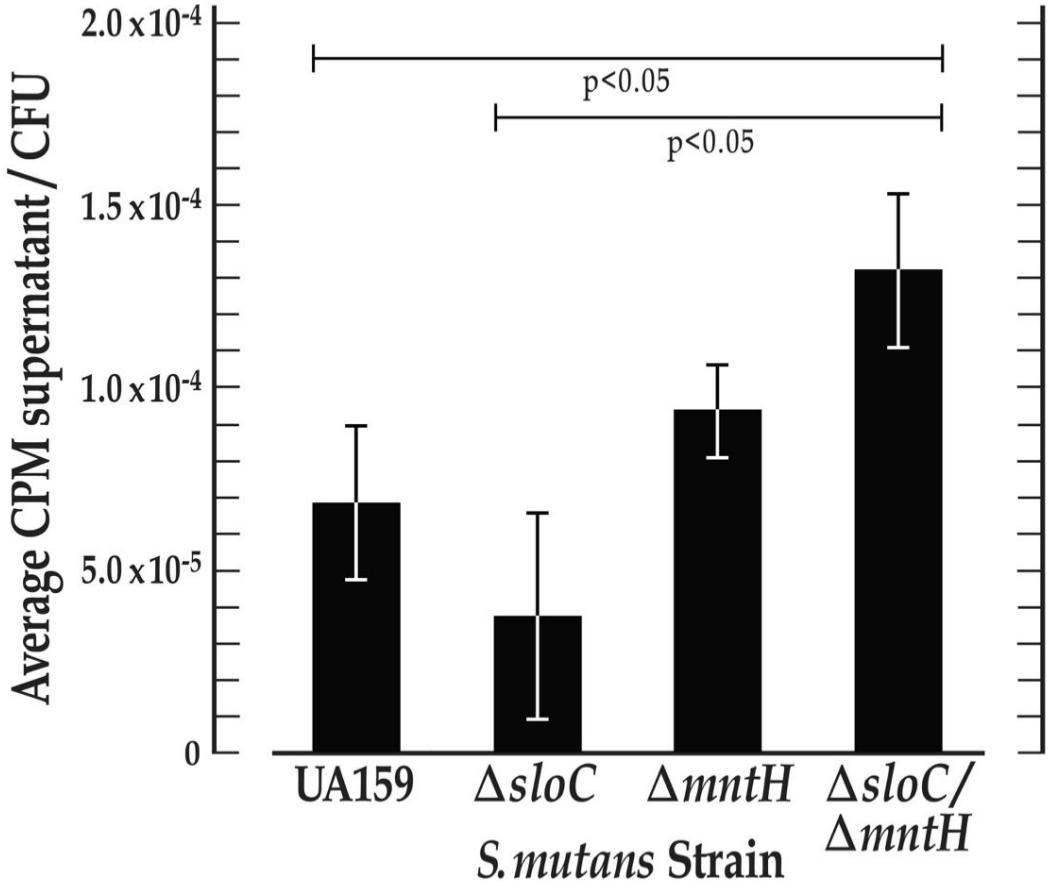

FIG 1 ^{54}Mn uptake experiments support SloC and MntH as the major compensatory transporters of manganese in *S. mutans*. ^{54}Mn uptake is significantly compromised in the *S. mutans* Δ*sloC*/Δ*mntH* double mutant when compared with that of its UA159 wild-type progenitor and its Δ*sloC* derivative (Kruskal-Wallis ANOVA, p<0.05, N=3) as indicated by heightened ^{54}Mn retention in the double mutant supernatant. All *S. mutans* cultures were grown overnight to within 0.005 absorbance units in the presence of ^{54}Mn or a 0.5M HCl control. The cell pellets and supernatants were separated by centrifugation, and CPM remaining in the culture supernatants was determined by liquid scintillation counting. The total number of CFUs in each sample was determined by serially diluting the control culture cell pellets and viable plate counting. The CPM in culture supernatants was divided by the total number of CFUs to normalize the output of the ^{54}Mn assay. Error bars denote the standard deviation of the mean.

biomass for the *mntH*/*sloABC* double mutant compared to its UA159 wild-type progenitor and single mutant derivatives (Fig. 2A and B). By contrast, the biofilm biomass of the Δ*mntH* and Δ*sloC* single mutants was not significantly different from that of the wild type, consistent with the compensatory roles of the MntH and SloABC Mn^{2+} uptake systems. Interestingly, scanning electron micrographs of *S. mutans* UA159, *ΔmntH*, *ΔsloC,* and *ΔmntHΔsloC* revealed biofilm architectures that were similar (Fig. 2C) with the exception of water channels that were somewhat obscured by the relatively thicker *ΔmntH* single and double mutant biofilms.

Characterization of the *S. mutans mntH* promoter region

To inform gene regulation at the *mntH* locus, we characterized the *mntH* promoter region by defining the transcription start site (TSS) from which we could predict SRE positioning relative to the −10 and −35 promoter elements. To this end, we conducted 5′ RACE experiments, the results of which support *mntH* transcription that begins at an adenosine residue located 32 bp upstream of the ATG start codon (Fig. 3). Based on the location of this adenosine residue, we predicted the positioning of the −10 and −35 *mntH* promoter elements, while taking into consideration the −10 and −35 consensus sequences in prokaryotes (20). The predicted −10 promoter element has a sequence that exactly matches that of the canonical prokaryotic sequence (TATAAT), while the predicted element positioned 35 nucleotides upstream of the TSS (TTAACA) deviates from the conserved −35 prokaryotic sequence (TTGACA), but only by a single nucleotide.

Regulation of the *S. mutans mntH* gene involves direct SloR binding to two SREs in the *mntH* promoter region

A previous report by Kajfasz et al. (7) described direct SloR binding to a 206 bp target probe that harbors the *S. mutans mntH* promoter sequence. To confirm this observation, we performed an EMSA experiment with the same 206 bp target probe, the results of which reveal a robust band shift (Fig. 4) when as little as 60 nM SloR was added to the reaction mixture. This band shift was abrogated by the addition of EDTA, consistent with a SloR-DNA interaction that is metal ion-dependent. Having demonstrated that SloR directly binds within the region of the *mntH* promoter, we performed biolayer interferometry to confirm this binding and to define a Kd value for the SloR-*mntH* interaction (Fig. S1). Interestingly, the Kd for SloR binding to a 90 bp probe of the *mntH* promoter is ~33 nM, which is similar to that for SloR binding to the 72 bp *sloABC* promoter (~31 nM) which was revealed in a parallel biolayer interferometry assay. Previous Kd determinations for SloR-*sloABC* binding derive from fluorescence anisotropy studies that similarly revealed a strong binding interaction (~30 nM) (17).

Additional EMSA experiments with serial deletion promoter fragments as target probes allowed us to home in on the specific region(s) in the *mntH* promoter region to which SloR binds (Fig. 4). Via visual inspection, Kajfasz et al. identified a palindrome in the *mntH* promoter region immediately downstream of the predicted −10 promoter element that resembles SREs A, B, and C that precede the *sloABC* genes on the UA159 chromosome (17). We were surprised by the results of EMSA experiments that do not support SloR binding to this sequence (Fig. 4). Instead, we observed robust band shifts with target probes that excluded this predicted SloR binding sequence and noted the absence of a band shift with probes that harbor only this predicted sequence (data not shown).

Interestingly, target probes that extend less than 75 bp upstream of the *mntH* translation start site failed to generate a band shift in these experiments, whereas those with more than 75 bp of upstream sequence generated a successful shift (Fig. 4A). We therefore focused our SRE search on a ~25 bp gap region where we identified a putative binding motif (TTTTAAGCATACTTAACA) comprised of a 6 bp half-palindrome (TTTTAA), a 6 bp intervening sequence, and another 6 bp imperfect half-palindrome, (TTAACA). This 6-6-6 motif, hereafter called SRE1, shares overlap with the *mntH* −35 promoter element. In fact, we observed robust band shifts when 60 nM SloR was added to reaction mixtures

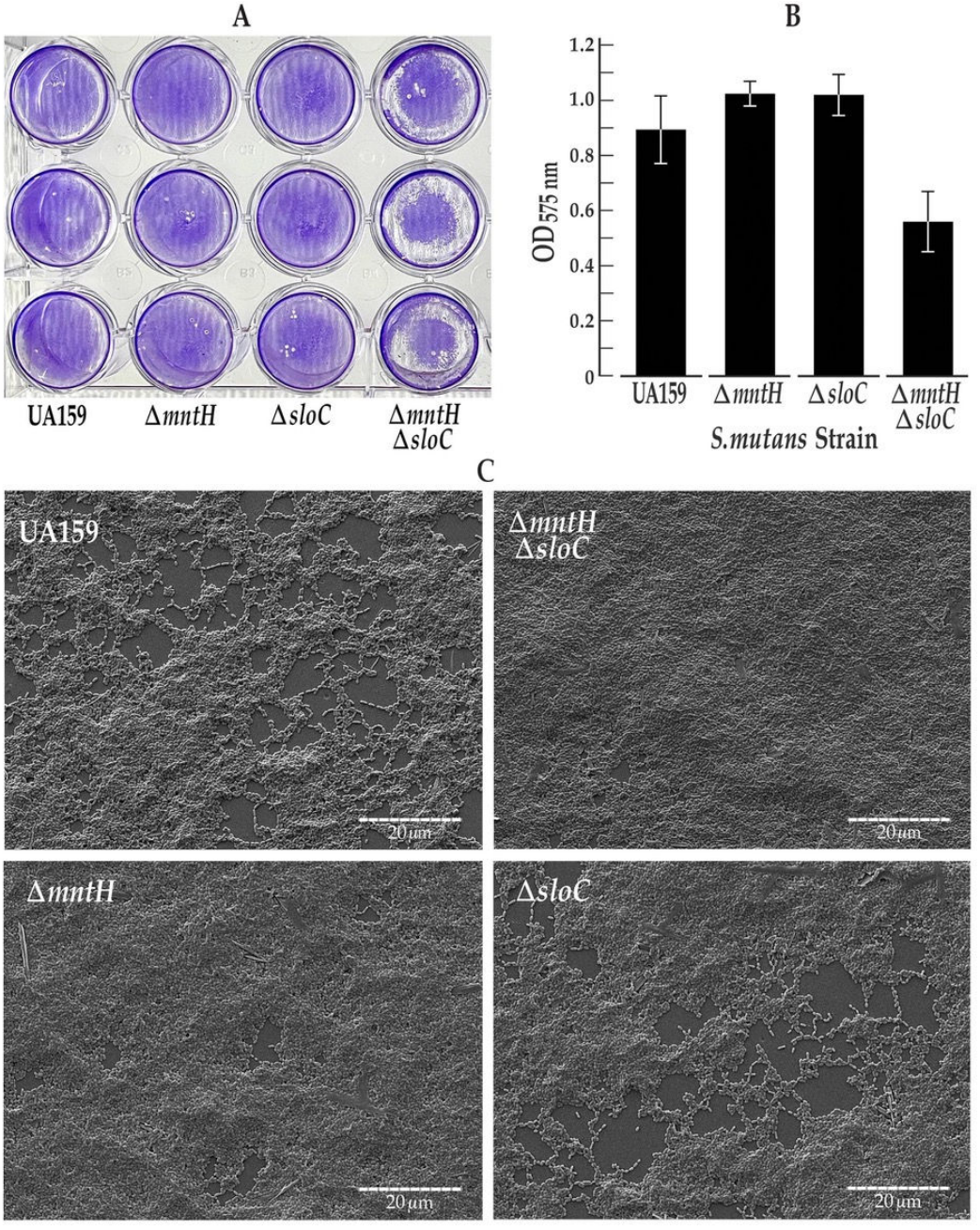

FIG 2 The *S. mutans* ΔmntHΔsloC mutant is compromised for adherence. *S. mutans* cultures were grown overnight to mid-logarithmic phase in 1:4 THYE media supplemented with 18mM glucose and 2mM sucrose. (a) The results of the crystal violet assay demonstrate reduced biofilm formation in the ΔmntHΔsloC mutant compared to the UA159 wild type and its single mutant derivatives. This phenotype reflects biofilms of the double mutant that were more fragile and less adherent to the polystyrene surface than those of the wild-type or single mutant variants. (b) Quantitative spectroscopy of crystal violet extracts from adherent biofilm cells reveals significantly compromised biofilm biomass for the ΔmntHΔsloC mutant compared to the UA159 wild-type strain (P = 0.02), and its isogenic ΔsloC (P = 0.004) and ΔmntH mutants (P = 0.002), as determined in two-tailed Student's t-tests. Error bars depict standard error of the mean. (c) Scanning electron micrographs of *S. mutans* UA159 and its ΔmntH and/or ΔsloC mutant derivatives grown on polystyrene coverslips reveal biofilm architectures that are similar. Most notably, the ΔmntH single and double mutants formed biofilms that appear thicker with water channels that were somewhat obscured compared to those present in the UA159 and ΔsloC biofilms. Otherwise, the biofilm architecture of the single and double mutants was indistinguishable from that of the UA159 wild-type progenitor. Shown in each electron micrograph are representative regions of the full biofilm.

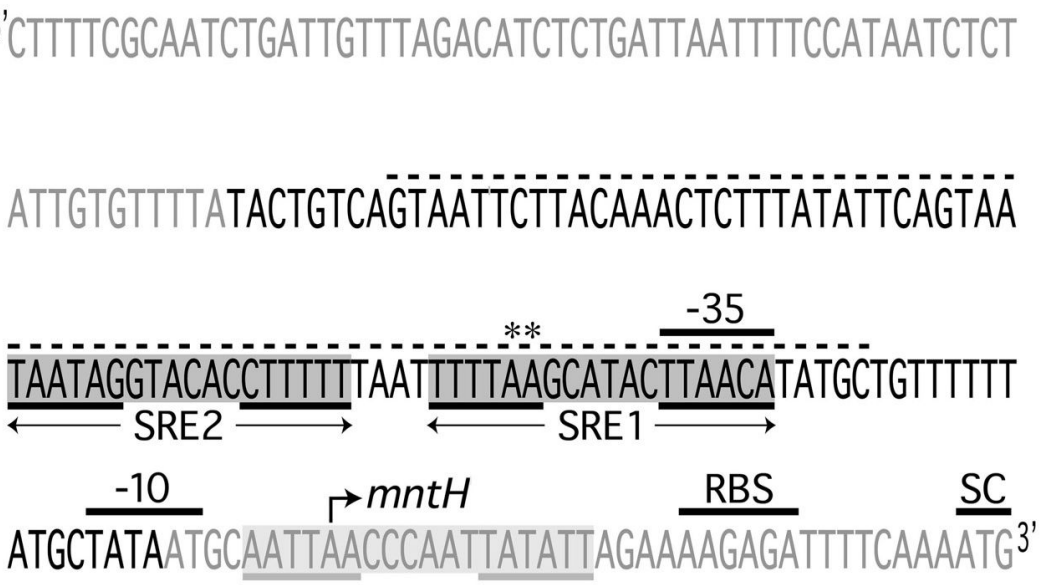

FIG 3 Organization of the *S. mutans mntH* promoter region. Shown are two SREs in the *mntH* promoter region that were predicted *in silico* and subsequently validated in DNA footprinting and gel shift experiments. SRE1 shares overlap with the −35 promoter element, and SRE2 is located 4bp adjacent to and upstream of SRE1. The SRE that was predicted by Kajfasz et al. (7) but not validated in this study is located downstream of SRE1 (highlighted in light gray). SREs 1 and 2 share a 6-6-6 binding motif, each composed of different imperfect inverted repeats (underlined). The region of DNA that was protected by SloR in DNA footprinting experiments is designated by the dashed line. The −35 and −10 promoter elements were predicted in 5′ RACE experiments in accordance with the identification of a transcription start site (bent arrow) which defines a 32-bp 5′ untranslated region. Also shown is the predicted ribosome binding site (RBS). Nucleotides designated in black comprise a 100-bp target probe that harbors both SREs and that was used in gel mobility shift assays. The asterisks indicate the two adenine residues that, when mutated, abrogate SloR binding in EMSA experiments. These same mutations were introduced into the *S. mutans* chromosome (generating GMS2027), which de-repressed *mntH* transcription.

containing target probes harboring SRE1, but not with probes that excluded SRE1 or any part thereof (Fig. 4B). To confirm SloR-SRE1 binding, we tested a 22 bp target probe that harbors the full 18 bp SRE1 sequence flanked by two additional base pairs on the 5′ and 3′ ends. Indeed, the 22 bp target probe was successfully shifted in these experiments with as little as 60 nM SloR (Fig. 4 and 8).

To identify the specific base pair contacts that are required for SloR-SRE1 binding, we performed EMSA experiments with SRE1 and several SRE1 mutant variants as target probes. Specifically, we tested an SRE1 derivative that harbors mutations in the left-most inverted repeat (IR) (TTTTccGCATACTTAACA) or in the right-most inverted repeat (TTTTAAGCATACggccCA) (data not shown). Both of these IR mutations abolished the band shift and speak to the importance of SRE 1, and more specifically, to adenine nucleotides for SloR binding.

The results of DNA footprinting experiments support an extended region of protected DNA in the *mntH* promoter that spans 76 base pairs and that can accommodate the binding of at least two SloR homodimers. The footprint includes SRE1 that was shifted by SloR in EMSA studies as well as a second SloR-binding sequence, likely TAATAGGTACACTTTTT, located 4 bp upstream of SRE1 (Fig. 5). We went on to investigate whether SloR binding to this upstream sequence, called SRE2, was at all dependent on SloR-SRE1 binding in EMSA experiments with promoter deletion target probes. We observed two distinct band shifts when SloR was added to a reaction mixture containing a wild-type probe with resident SRE1 and SRE2 sequences, consistent with the presence of more than a single SloR-binding site in the *mntH* promoter region (Fig. 6). ImageJ analysis revealed a relative band intensity ratio consistent with more prevalent SloR binding to both SREs 1 and 2 as opposed to SRE 1 alone (1.3–0.03 AU, respectively). A reaction

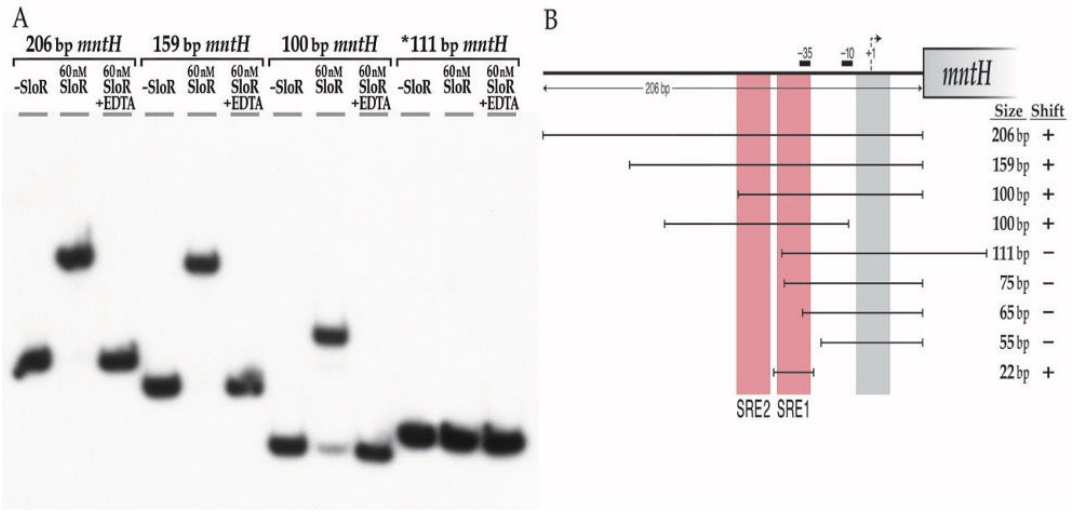

FIG 4 The *S. mutans* SloR protein binds to the *mntH* promoter fragment. (a) Amplicons that extend 206-bp, 159-bp, and 100-bp upstream of the *mntH* coding sequence are shifted by SloR. All three of these deletion fragments, including the 100-bp probe, span a region upstream of the *mntH* transcription start site that does not include the transcription start site. Abrogation of the band shifts by EDTA supports the SloR-DNA interaction as metal ion-dependent. Interestingly, a 111-bp probe that extends 75 bp upstream of the *mntH* start codon and 36 bp into the *mntH* coding sequence was not shifted by SloR (see *). (b) Shown are serial deletion fragments of the 206 bp *mntH* locus that were used as probes in EMSA experiments to reveal the region of SloR binding within the *S. mutans mntH* promoter region. The vertical shading in red indicates the positioning of SREs 1 and 2 relative to the predicted −10 and −35 promoter elements. Shown by the vertical gray bar is a predicted SRE to which SloR does not bind. The (+) designation indicates robust shifting of the probe by 60 nM SloR in EMSA experiments; the (–) sign indicates the absence of a shift. Robust band shifts were generated with probes harboring SRE1 but not with probes that excluded this SRE or any part of this binding motif.

mixture containing 60 nM SloR and a target probe with a mutation in SRE1 (but wild-type SRE2) revealed a gel shift pattern consistent with continued SloR binding to SRE2. A probe with a mutation in SRE2 (but wild-type SRE1) again revealed two band shifts consistent with SloR binding to at least two SREs. ImageJ quantification revealed a high-intensity band shift that was compromised for SloR binding when SRE2 was mutated (2.4 vs. 0.7 arbitrary units) as opposed to when SRE 2 was present in its wild-type configuration (1.3 vs. 0.03 AU). That the upper band shift is compromised when SRE2 is altered supports SloR binding to SREs 1 and 2 that is cooperative. The existence of an additional SRE upstream of SRE2 cannot be ruled out, however. Taken together, these results support the presence of at least two SREs in the *S. mutans mntH* promoter region, to which SloR appears to be binding cooperatively, favoring binding to SRE1 over SRE2.

Kd values defined by biolayer interferometry are consistent with cooperative SloR binding at the *mntH* locus and implicate a significantly higher SloR binding affinity (and hence a lower Kd) for the SloR-SRE1 interaction than for that of SloR binding to SRE2. A 22 bp probe that harbors only SRE1 binds to SloR in these experiments, whereas 22 bp probes that harbor SRE2 alone do not (Fig. S2). These results corroborate the results of EMSA, demonstrating that only SRE1 can support SloR binding when provided as the sole binding site, *in vitro*.

Mutations in SRE1 and/or SRE2 de-repress transcription of the *S. mutans mntH* gene *in vivo*

We investigated the impact of wild-type and mutant SRE1 and SRE2 variants on *mntH* transcription in real-time semi-quantitative PCR (qRT-PCR) studies. Specifically, we monitored transcription of the *mntH* gene in the wild-type UA159 strain and in its mutant derivatives GMS2027, GMS2028, and GMS2029. *S. mutans* GMS2027 harbors two adenine substitutions in the leftmost IR of SRE1 (changed to cytosines) to mimic the test probe that was characterized for SloR binding in EMSA experiments. The qRT-PCR results revealed 4.5-fold derepression of *mntH* transcription in GMS2027 compared to

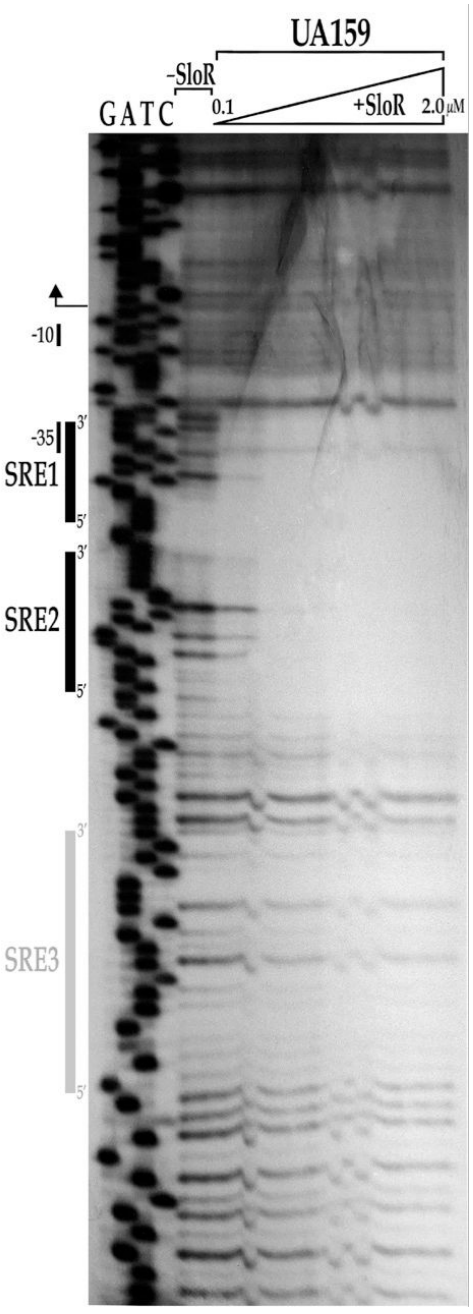

FIG 5 SloR protects a region in the *mntH* promoter harboring at least two SREs. SloR protects a 76-bp region of DNA upstream of the *mntH* coding sequence that includes SREs 1 and 2 as well as the −35 promoter region. A third footprint is implicated upstream of SRE2 but warrants further investigation. A 291-bp amplicon on which the *mntH* promoter is resident was generated with a 5′-end labeled forward primer and a corresponding reverse primer. The radio-labeled amplicon was used in binding reactions with increasing amounts of SloR up to 2 µM. Each reaction along with no protein controls were digested with RQ1 DNase I and resolved on an 8% urea-containing polyacrylamide gel. Shown within the region of protection are two SREs (indicated by the vertical black bars) and possibly a third footprint (indicated by the vertical light gray bar), supporting the presence of at least two SREs. The positioning of the −10 and −35 promoter regions are also shown relative to the positioning of the *mntH* transcription start site (bent arrow).

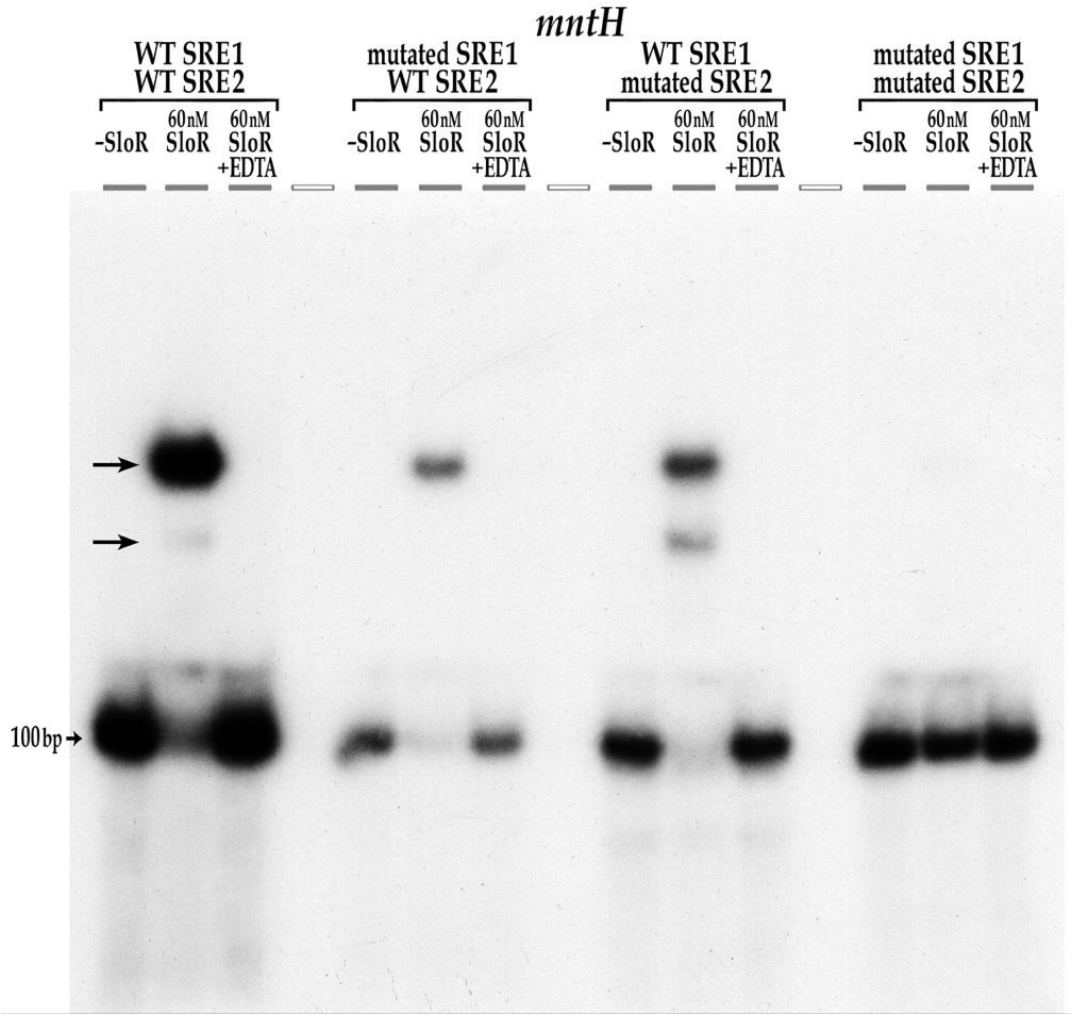

FIG 6 SRE1 mutant variants resident on a 100-bp target probe disrupt cooperative SloR binding to the *mntH* promoter in EMSA experiments. A 100-bp probe that harbors wild-type SREs 1 and 2 produces two visible band shifts (arrows) when 60nM SloR is added to the reaction mixture. The same 100-bp probe with two A-to-C transversion mutations in SRE1 (TTTTccGCATACTTAACA) abrogated the lower of the two band shifts. Maintenance of the upper band supports persistent binding of a SloR homodimer to SRE2. Interestingly, the 100-bp probe with mutations in SRE2 only (TAATtcGTACACCTTTTT) returns the band shift pattern to that of wild type, only with different relative band intensities. This result, which supports compromised SloR binding to SRE 1 when the sequence of SRE2 is mutated, is consistent with cooperative binding of SloR to SREs 1 and 2. Given the relative band intensities when SRE2 is variant, one cannot rule out the possibility of an additional SRE upstream of SRE2. We predict SloR binding to any additional upstream SREs would be cooperative and dependent on SloR binding to SREs 1 and 2. As expected, the abrogation of both band shifts occurs when mutations are introduced into both SREs 1 and 2. The addition of EDTA to the reaction mixtures abrogates the band shift, indicating that the observed SloR-DNA interactions are metal ion-dependent.

its UA159 progenitor (Fig. 7), indicating the essentiality of adenine residues within SRE1 in SloR binding. Transcription of the *mntH* gene in *S. mutans* GMS2028, which harbors two transversion mutations (AG to TC) in the leftmost IR of SRE2, was de-repressed nearly threefold, underscoring the involvement of SRE2 in SloR binding to the *mntH* promoter region. Finally, *mntH* transcription in the GMS2029 SRE variant, which harbors both aforementioned mutations in SRE1 and SRE2, respectively, was de-repressed more than threefold. This de-repression (owing to compromised SloR-DNA binding) supports the essentiality of SRE1 and SRE2 for SloR binding and *mntH* gene regulation.

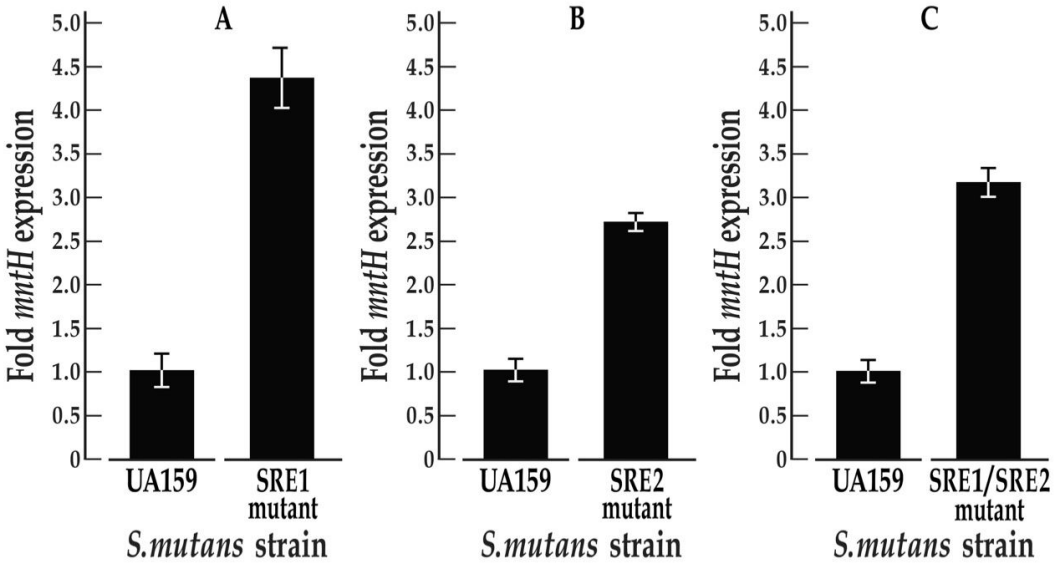

FIG 7 Impact of SRE mutant variants on *S. mutans mntH* transcription *in vivo*. Semi-quantitative real-time PCR experiments were performed in triplicate with the wild-type UA159 *S. mutans* strain and its *mntH* SRE mutant derivatives. The expression of *mntH* was normalized against that of an *hk11* housekeeping gene. (a) The transcription of *mntH* was significantly de-repressed ~4.5-fold in the SRE1 mutant variant (GMS2027), compared to the UA159 wild-type strain. Transcription of *mntH* in the SRE2 mutant variant (GMS2028) and in the SRE1/SRE2 double variant (GMS2029) was also de-repressed compared to wild type by ~3-fold. The former harbors two transversion mutations in SRE2, and the latter harbors transversion mutations in both SREs 1 and 2. Shown is the mean *mntH* expression ± standard deviation that derives from three technical replicates in each of three independent experiments.

The spacer sequence that separates the inverted repeats (IRs) within an SRE is important but not sufficient for SloR-SRE binding

We conducted EMSA experiments with SRE target probes harboring aberrant IR or spacer sequences to determine whether the SRE spacer in the binding motif is important for SloR-SRE binding. We pursued these experiments because of the degeneracy we observed in the IRs that flank SREs 1 and 2 despite SloR binding to these sequences. Specifically, we constructed a 22 bp target probe with resident SRE1 IR sequences and a variant 6 bp spacer region. Interestingly, alterations to the SRE1 spacer abolished the robust SloR-SRE1 band shift that we had observed previously with the wild-type SRE1 sequence (Fig. 8). That the SloR-SRE1 band shift was compromised by introducing a unique spacer speaks to the importance of the spacer motif in SloR-SRE binding. We extended these studies to determine whether the SRE1 spacer alone could be sufficient for SloR binding. We did this by generating a target probe composed of IR sequences that we know do not engage SloR with the SRE1 spacer that we know does. When SloR was added to this probe combination, a band shift was still not observed (data not shown). Taken together, these findings support an important role for the SRE spacer in SloR binding but indicate that the spacer alone is not sufficient for the SloR-SRE interaction (Fig. 8).

DISCUSSION

Manganese is an essential micronutrient that promotes the survival and pathogenicity of numerous lactic acid bacteria, including *S. mutans* (10). This divalent cation is most widely known as a cofactor for the detoxifying superoxide dismutase (MnSOD) in *S. mutans* that protects the bacterium against oxidative stress (6). Reports in the literature describe SloABC-mediated metal ion transport as the main manganese uptake system in this oral pathogen, although redundant systems have been reported (17). The focus of the present study is on the MntH manganese permease in *S. mutans,* which Kajfasz et al. (7) identified as an ancillary transporter of Mn^{2+} via inductively coupled plasma

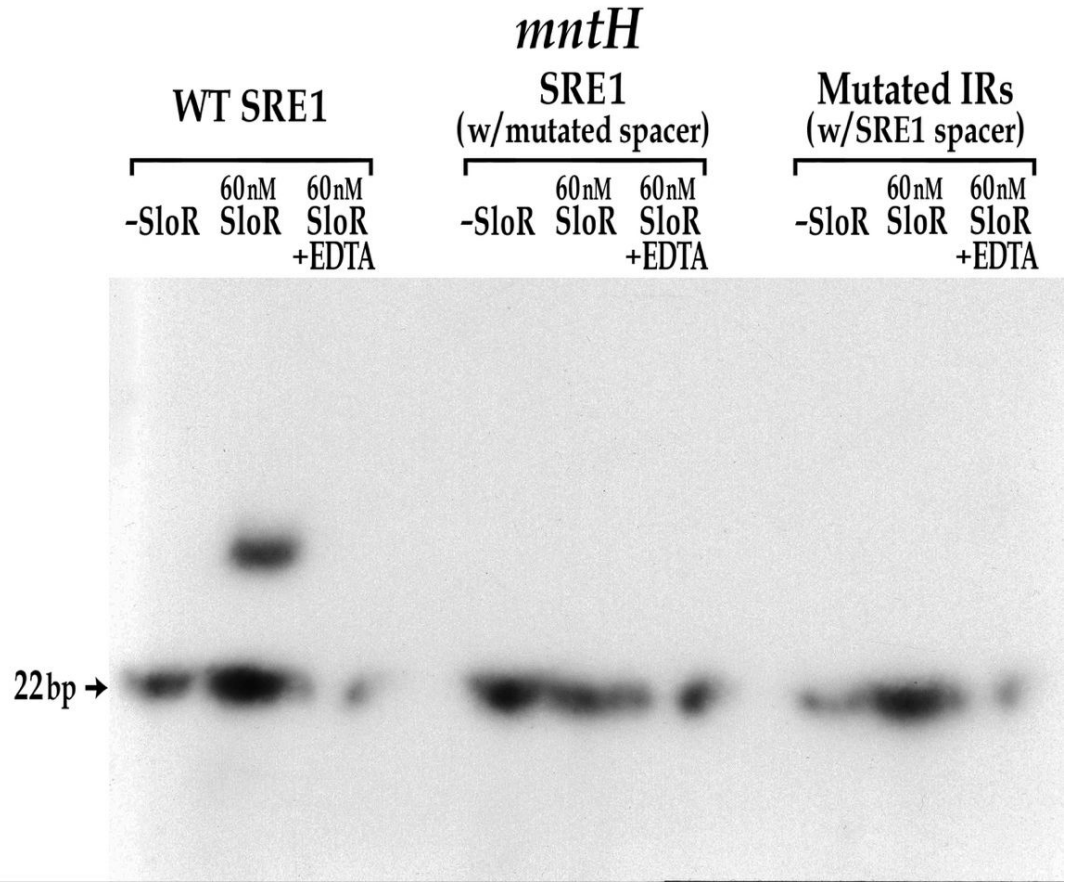

FIG 8 The SRE1 spacer region is important but not sufficient for SloR binding. Wild-type SRE1 (TTTTAAGCATACTTAACA) in the *mntH* promoter region was successfully shifted by 60nM SloR. By contrast, the same 22-bp probe with a different spacer sequence (TTTTAACCCAATTAACA) was not shifted by SloR. The same 22-bp probe with the SRE1 spacer flanked by unique IR sequences (AATTAAGCATACTATATT) also failed to generate a band shift. Abrogation of the band shifts by EDTA supports a SloR-DNA interaction that is metal ion-dependent.

optical emission spectrometry (ICP-OES). In the present study, we performed ^{54}Mn uptake experiments with *S. mutans* cells grown in a Mn-replete medium. ^{54}Mn accumulation was significantly heightened in supernatants of the *ΔmntHΔsloC* double mutant compared to wild type, indicating that the SloABC and MntH metal ion transport systems represent the main importers of manganese in *S. mutans*. Compensatory roles for SloABC and MntH in manganese transport are also implicated by ^{54}Mn accumulation in culture supernatants of the *mntH* and *sloC* single mutants that are not significantly different, and further supported by the results of crystal violet release assays which reveal biofilm biomasses for the *sloABC* and *mntH* single mutants that are indistinguishable from one another. We propose that the redundancy of manganese uptake systems in *S. mutans* promotes its fitness by allowing it to maintain intracellular Mn^{2+} homeostasis despite the highly transient environment of the human mouth, particularly during periods of feast and famine when Mn^{2+} levels are fluctuating.

Manganese uptake in *S. mutans* occurs primarily via the SloABC system where it is subject to SloR control. Previous work in our laboratory supports SloR binding to so-called SloR recognition elements, or SREs, in the *sloABC* promoter region which represses transcription of the downstream *sloABC* operon (17), presumably via a promoter exclusion mechanism. The results of previously published DNA footprinting assays (17) confirm that SloR binding to the *sloABC* promoter engages each of three inverted hexameric repeat units, each separated by 4 bp. Specifically, the three SREs span

72 bp of DNA in the region and share overlap with the −10 and −35 promoter elements. Each SRE includes an AATTAA IR sequence separated by a 6 bp spacer, comprising a 6-6-6 binding motif. Transcription of the *S. mutans mntH* gene is also subject to SloR control. The results of EMSA experiments support direct SloR binding to a 206 bp *mntH* promoter fragment at protein concentrations as low as 60 nM. In fact, the binding studies reported herein support two SloR binding sites in the *mntH* promoter within 135 bp of the TSS. SRE1 and its IRs TTTTAA and TTAACA share overlap with the −35 *mntH* promoter element, suggesting that SloR represses *mntH* via steric hindrance (21), a mechanism commonly observed among SloR homologs (22–24). Interestingly, the SRE1 IRs deviate from the IRs of the *sloABC* SRE-B by 4 bp, and the IRs of SRE 2 deviate from those of the *sloABC* SRE-B by six base pairs. Consistent with the EMSA findings are the results of biolayer interferometry experiments that reveal SRE 1 as having the most robust affinity for binding SloR independently. By contrast, SRE 2 alone does not bind SloR as robustly without the stabilizing effect of the SloR-SRE1 interaction, as demonstrated in gel mobility shift experiments.

The introduction of site-specific mutations into SRE1 abrogated SloR-SRE1 binding but maintained a shifting pattern consistent with SloR binding to more than a single SRE. By contrast, mutations in SRE2 maintained the wild-type gel shift pattern, only with different relative band intensities that speak to a loss of cooperative SloR binding but binding nevertheless to SRE 1 and possibly an additional SRE upstream. Mutations in both SREs 1 and 2 abrogated both band shifts. Taken together, these findings support the presence of at least two SREs in the *mntH* promoter region and are consistent with cooperative SloR-SRE binding that favors an interaction with SRE1 before engaging with SRE 2. This is further supported by the biolayer interferometry results.

We reported previously on cooperative SloR-SRE binding at the *sloABC* promoter (17). Experiments conducted more recently in our laboratory lend even further support to cooperative binding to the promoters that SloR regulates. That is, we demonstrated that C-terminal interactions between adjacent SloR homodimers facilitate SloR-SRE binding and that these interactions are mediated by a quintet of amino acids, including phenylalanine 187 (data not shown). Substituting this phenylalanine residue in the C-terminal FeoA domain of the SloR protein with a conservative (F187E) or non-conservative (F187A) glutamine or alanine residue, respectively, compromised the SloR-SRE interaction in EMSA experiments and significantly de-repressed *sloABC* transcription in expression profiling studies, consistent with the cooperative binding of SloR homodimers to adjacent SREs (data not shown). Herein, we report similar cooperative binding for SloR to two adjacent SREs (SREs 1 and 2) in the *mntH* promoter. Cooperative binding at the *S. mutans mntH* locus is further supported by a recent study of MntR, a SloR homolog in *Bacillus subtilis* that binds with cooperativity to the *mneP* promoter (25).

Since SloR binding to SRE1 blocks −35 promoter access to RNA polymerase, we anticipated transcriptional repression of the downstream *mntH* gene in expression profiling experiments. We propose SloR binding to both SRE1 and SRE2 on the *S. mutans* chromosome may fine-tune this repression, presumably upon SloR binding to DNA with varying affinities (21). Notably, *in silico* analysis of the *S. mutans* UA159 genome revealed palindromic IR sequences that comprise a putative SRE near the *mntH* −10 promoter element. The IRs of this predicted SRE deviate from the *sloABC* IR sequences by only two base pairs (AATTAA and TTAATT for *sloABC* versus AATTAA and TATATT for *mntH*). Yet, our experimental results do not support SloR binding to this site, despite sharing sequence similarity with the high affinity SRE (Kd = 30 nM) at the *sloABC* locus.

The results of biolayer interferometry reveal similar Kd values for SloR binding at the *mntH* and *sloABC* loci. Owing to the sequence divergence between SRE1 and the canonical SRE that precedes the *sloABC* operon, we did not anticipate the near equivalent binding affinities that we observed with SloR. Rather, we anticipated a weaker SloR-SRE1-binding interaction at the *mntH* locus, and hence more relaxed *mntH* transcription that would align with how an ancillary Mn^{2+} permease might fine-tune metal ion import that is otherwise largely determined by SloR-mediated gene

control. Instead, the experimental findings reveal SloR binding sequences that can vary significantly and still engage SloR with high affinity. Taken together, these findings support a SloR-SRE interaction in the *S. mutans mntH* promoter region that is likely not wholly sequence-dependent.

We were also intrigued by the evidence that supports an integral role for the SRE spacer in SloR binding. Specifically, we were surprised by the relatively robust binding that we observed for SloR and SRE1 despite the degeneracy of the interrupted palindrome. This led us to hypothesize that the IRs alone may not be fully accountable for SloR-SRE binding and that the 6 bp spacer region may be involved. We performed a spacer mutation experiment to address this hypothesis by substituting the SRE1 spacer with a random sequence of nucleotides (Fig. 8). This spacer alteration effectively abolished SloR binding, demonstrating that the spacer region contributes to SloR binding, and that perfect consensus IRs alone cannot fully explain the SloR-SRE interaction.

Based on what is known about other homodimeric proteins belonging to the DtxR family of metalloregulators, SloR engages the N-terminal helix-turn-helix (H-T-H) motif of each of its monomeric subunits with the major groove of DNA (21). Given that the length of the SRE is 18 bp and that 10.4 bp are required for a single turn of B-DNA, we deduced that the SRE IRs would align with the major groove of the DNA and that the spacer region would align with the minor groove. Although the spacer does not make direct contact with SloR, growing evidence that supports spacer involvement in SloR-DNA binding led us to consider the shape of the DNA and the span of the SloR homodimer in modeling the SloR-SRE binding interaction. Accordingly, we propose that the spacer sequence influences DNA conformation and hence, by inference, the location and accessibility of the SRE IRs to the SloR protein. It is also possible, however, that SloR binding via direct base pair contacts in the major groove (known as direct readout) is less important than previously thought, and that SloR instead interacts with the DNA backbone. Hence, how the spacer impacts the DNA backbone could influence SloR binding affinity as much as the IR sequence (indirect readout). Indirect readout involving SloR recognition of the DNA backbone is reminiscent of the way IdeR in *Mycobacterium* interacts with its DNA target sequence. This IdeR-DNA binding mechanism has its basis in sequence-dependent DNA backbone recognition rather than via base pair contacts with the DNA (26).

In summary, the results of the present study support at least two redundant pathways for manganese import in *S. mutans* that are mediated by the SloABC and MntH systems, and that we believe fine-tune metal ion uptake and maximize bacterial fitness. The identification of at least two SREs in the *mntH* promoter region with some degeneracy, when compared with the canonical SREs that precede the *S. mutans sloABC* promoter, begs the question of whether sequence dependence is the whole story. Accumulating evidence that points to the involvement of the SRE spacer in SloR binding can expand our understanding of the SloR-SRE interaction at the *sloABC* and *mntH* promoters, and potentially others across the *S. mutans* genome. An improved understanding of where and how SloR binds and regulates its gene targets is important because it can inform the development of therapeutics that target the SloR-DNA-binding interface, with the ultimate goal of alleviating or preventing dental caries.

ACKNOWLEDGMENTS

We thank Gary Nelson for figure preparation and Michael Freeman, and Will Nemeth for their valuable contributions to this research.

This research was supported by the National Institutes of Health (NIH), grant R01DE014711 to G.A.S., the Middlebury College Senior Research Supplement Fund, and the Middlebury College Department of Biology.

AUTHOR AFFILIATIONS

[1]Program in Molecular Biology & Biochemistry, Department of Biology, Middlebury College, Middlebury, Vermont, USA
[2]Department of Restorative Dentistry, School of Dentistry, Oregon Health & Science University, Portland, Oregon, USA

PRESENT ADDRESS

Myrto Ziogas, Department of Stem Cell and Regenerative Biology, Harvard University, Cambridge, Massachusetts, USA
Igor Todorovic, Department of Microbiology and Immunology, Geisel School of Medicine, Dartmouth College, Hanover, New Hampshire, USA

AUTHOR ORCIDs

India Drummond http://orcid.org/0000-0003-3566-634X
Hui Wu https://orcid.org/0000-0003-1694-3954
Grace Spatafora http://orcid.org/0000-0003-2043-4853

FUNDING

Funder	Grant(s)	Author(s)
National Institutes of Health	R01DE014711	Myrto Ziogas India Drummond Igor Todorovic Katie Kraczkowsky Yiran Han Hua Zhang Hui Wu Grace Spatafora
Middlebury College Senior Research Supplement Fund		Myrto Ziogas India Drummond Igor Todorovic Katie Kraczkowsky Yiran Han Hua Zhang Hui Wu Grace Spatafora
Middlebury College Department of Biology		Myrto Ziogas India Drummond Igor Todorovic Katie Kraczkowsky Yiran Han Hua Zhang Hui Wu Grace Spatafora

AUTHOR CONTRIBUTIONS

Myrto Ziogas, Conceptualization, Investigation, Methodology, Writing – original draft, Writing – review and editing | India Drummond, Conceptualization, Investigation, Methodology, Writing – original draft, Writing – review and editing | Igor Todorovic,

Investigation, Methodology, Writing – original draft | Katie Kraczkowsky, Investigation, Methodology, Writing – original draft | Yiran Han, Investigation, Methodology | Hua Zhang, Investigation, Writing – review and editing | Hui Wu, Methodology, Supervision | Grace Spatafora, Conceptualization, Formal analysis, Funding acquisition, Project administration, Supervision, Writing – original draft, Writing – review and editing

ADDITIONAL FILES

The following material is available online.

Supplemental Material

Supplemental figure legends (JB00470-24-s0001.docx). Legends for Figures S1 and S2.
Figure S1 (JB00470-24-s0002.tif). Binding affinity determinations for the *S. mutans* SloR protein and the *sloABC* and *mntH* promoter probes via biolayer interferometry.
Figure S2 (JB00470-24-s0003.tif). Binding affinity determinations for the *S. mutans* SloR protein and 22-bp probes in the *mntH* promoter region harboring SRE1 and 2 by biolayer interferometry.
TABLE S1 (JB00470-24-s0004.docx). Primers and oligonucleotides used in this study

REFERENCES

1. Kilian M, Chapple ILC, Hannig M, Marsh PD, Meuric V, Pedersen AML, Tonetti MS, Wade WG, Zaura E. 2016. The oral microbiome - an update for oral healthcare professionals. Br Dent J 221:657–666. https://doi.org/10.1038/sj.bdj.2016.865
2. Aas JA, Paster BJ, Stokes LN, Olsen I, Dewhirst FE. 2005. Defining the normal bacterial flora of the oral cavity. J Clin Microbiol 43:5721–5732. https://doi.org/10.1128/JCM.43.11.5721-5732.2005
3. Takahashi N, Nyvad B. 2011. The role of bacteria in the caries process: ecological perspectives. J Dent Res 90:294–303. https://doi.org/10.1177/0022034510379602
4. Anderson AC, Rothballer M, Altenburger MJ, Woelber JP, Karygianni L, Lagkouvardos I, Hellwig E, Al-Ahmad A. 2018. *In-vivo* shift of the microbiota in oral biofilm in response to frequent sucrose consumption. Sci Rep 8:14202. https://doi.org/10.1038/s41598-018-32544-6
5. Lemos JA, Palmer SR. 2019. The biology of *Streptococcus mutans*. Microbiol Spectr 7. https://doi.org/10.1128/microbiolspec.GPP3-0051-2018
6. Martin ME, Byers BR, Olson MO, Salin ML, Arceneaux JE, Tolbert C. 1986. A *Streptococcus mutans* superoxide dismutase that is active with either manganese or iron as A cofactor. J Biol Chem 261:9361–9367.
7. Kajfasz JK, Katrak C, Ganguly T, Vargas J, Wright L, Peters ZT, Spatafora GA, Abranches J, Lemos JA. 2020. Manganese uptake, mediated by SloABC and MntH, is essential for the fitness of *Streptococcus mutans*. mSphere 5:e00764-19. https://doi.org/10.1128/mSphere.00764-19
8. Bosma EF, Rau MH, van Gijtenbeek LA, Siedler S. 2021. Regulation and distinct physiological roles of manganese in bacteria. FEMS Microbiol Rev 45:fuab028. https://doi.org/10.1093/femsre/fuab028
9. Hood MI, Skaar EP. 2012. Nutritional immunity: transition metals at the pathogen-host interface. Nat Rev Microbiol 10:525–537. https://doi.org/10.1038/nrmicro2836
10. Juttukonda LJ, Skaar EP. 2015. Manganese homeostasis and utilization in pathogenic bacteria. Mol Microbiol 97:216–228. https://doi.org/10.1111/mmi.13034
11. Spatafora G, Corbett J, Cornacchione L, Daly W, Galan D, Wysota M, Tivnan P, Collins J, Nye D, Levitz T, Breyer WA, Glasfeld A. 2015. Interactions of the metalloregulatory protein SloR from *Streptococcus mutans* with Its metal ion effectors and DNA binding site. J Bacteriol 197:3601–3615. https://doi.org/10.1128/JB.00612-15
12. Xie Z, Okinaga T, Qi F, Zhang Z, Merritt J. 2011. Cloning-independent and counterselectable markerless mutagenesis system in *Streptococcus mutans*. Appl Environ Microbiol 77:8025–8033. https://doi.org/10.1128/AEM.06362-11
13. Sambrook J, Russell DW. 2006. Purification of nucleic acids by extraction with phenol:chloroform. Cold Spring Harb Protoc 2006:pdb. https://doi.org/10.1101/pdb.prot4455
14. Crepps SC, Fields EE, Galan D, Corbett JP, Von Hasseln ER, Spatafora GA. 2016. The SloR metalloregulator is involved in the *Streptococcus mutans* oxidative stress response. Mol Oral Microbiol 31:526–539. https://doi.org/10.1111/omi.12147
15. Haswell JR, Pruitt BW, Cornacchione LP, Coe CL, Smith EG, Spatafora GA. 2013. Characterization of the functional domains of the SloR metalloregulatory protein in *Streptococcus mutans*. J Bacteriol 195:126–134. https://doi.org/10.1128/JB.01648-12
16. Ruxin TR, Schwartzman JA, Davidowitz CR, Peters Z, Holtz A, Haney RA, Spatafora GA. 2021. Regulatory involvement of the PerR and SloR metalloregulators in the *Streptococcus mutans* oxidative stress response. J Bacteriol 203:e00678-20. https://doi.org/10.1128/JB.00678-20
17. Monette P, Brach R, Cowan A, Winters R, Weisman J, Seybert F, Goguen K, Chen J, Glasfeld A, Spatafora G. 2018. Autoregulation of the *Streptococcus mutans* SloR metalloregulator is constitutive and driven by an independent promoter. J Bacteriol 200:00214–00218. https://doi.org/10.1128/JB.00214-18
18. Rolerson E, Swick A, Newlon L, Palmer C, Pan Y, Keeshan B, Spatafora G. 2006. The SloR/Dlg metalloregulator modulates *Streptococcus mutans* virulence gene expression. J Bacteriol 188:5033–5044. https://doi.org/10.1128/JB.00155-06
19. Liu C, Zhang H, Peng X, Blackledge MS, Furlani RE, Li H, Su Z, Melander RJ, Melander C, Michalek S, Wu H. 2023. Small molecule attenuates bacterial virulence by targeting conserved response regulator. MBio 14:e0013723. https://doi.org/10.1128/mbio.00137-23
20. Szoke PA, Allen TL, deHaseth PL. 1987. Promoter recognition by *Escherichia coli* RNA polymerase: effects of base substitutions in the -10 and -35 regions. Biochemistry 26:6188–6194. https://doi.org/10.1021/bi00393a035
21. Browning DF, Busby SJW. 2016. Local and global regulation of transcription initiation in bacteria. Nat Rev Microbiol 14:638–650. https://doi.org/10.1038/nrmicro.2016.103
22. Toukoki C, Gold KM, McIver KS, Eichenbaum Z. 2010. MtsR is a dual regulator that controls virulence genes and metabolic functions in addition to metal homeostasis in the group A *Streptococcus*. Mol Microbiol 76:971–989. https://doi.org/10.1111/j.1365-2958.2010.07157.x
23. Posey JE, Hardham JM, Norris SJ, Gherardini FC. 1999. Characterization of a manganese-dependent regulatory protein, TroR, from *Treponema pallidum*. Proc Natl Acad Sci U S A 96:10887–10892. https://doi.org/10.1073/pnas.96.19.10887
24. Zheng C, Wei M, Qiu J, Jia M, Zhou X, Jiao X. 2021. TroR negatively regulates the TroABCD system and is required for resistance to metal toxicity and virulence in *Streptococcus suis*. Appl Environ Microbiol 87:e01375. https://doi.org/10.1128/AEM.01375-21
25. Shi H, Fu Y, Kodyte V, Andreas A, Sachla AJ, Miller K, Shrestha R, Helmann JD, Glasfeld A, Ahuja S. 2024. Structural basis for transcription activation through cooperative recruitment of MntR. bioRxiv:2024.06.28.601288. https://doi.org/10.1101/2024.06.28.601288

26. Marcos-Torres FJ, Juniar L, Griese JJ. 2023. The molecular mechanisms of the bacterial iron sensor IdeR. Biochem Soc Trans 51:1319–1329. https://doi.org/10.1042/BST20221539